Application of Acoustic Emission Technique for Indirect Measurement of Vertical Insitu Stress in Rock Mass – A Lab-Scale Study

P. B. Choudhury*
A. K. Chakraborty*
S. K. Singh**
A. K .Raina*
M. Ramulu*
A. Sinha*
A. Haldar*
and
J. L. Jethwa*

**Central Mining Research Institute Regional Centre*
3rd Floor, MECL Complex, Seminary Hills
Nagpur – 440 001, India
Email: cmrirc@satyam.net.in

***Central Mining Research Institute*
Barwa Road, Dhanbad – 826 001, India

ABSTARCT

Rocks when subjected to cyclic loading and unloading emit acoustic signals. Without stress, there is no emission. An acoustic emission (AE) inspection is usually carried out during controlled loading of the samples.

In this paper an attempt has been made to determine the maximum insitu stress to which the rock has been subjected to, due to stress variations since its formation using Kaiser and Felicity effect. Samples of sandstone and compact basalt's obtained from vertically drilled boreholes were subjected to cyclic compressive loading and unloading. An indirect evaluation technique of insitu stress using acoustic emission has been investigated and results are compared with other methods. It has been found that the vertical insitu stress results obtained by using acoustic emission tool matches with the values obtained by other methods.

Key Words: Acoustic emission, Felicity Ratio, Kaiser Effect, Insitu stress, Onset stress

1. INTRODUCTION

The deformation and failure of rock is generally associated with the growth and coalescence of cracks. Such phenomena generate relatively well defined, low level seismic activity, which when tapped and analysed act as an important tool in providing vital information regarding the existing stress levels. In general this low-level seismic activity is denoted as acoustic emission (AE)/ micro-seismic activity (MS). Acoustic emissions are elastic waves generated in conjunction with energy release during micro-cracks, crack propagation, pore collapsing and internal deformation in rocks.

The study of AE has developed into an increasingly popular form of non-destructive testing. The technique has long been employed in pressure vessel testing and an American Society for Testing and Materials (ASTM) method is widely used in the nuclear industry for this purpose. AE events have been used, especially in Japan (Glaser and Nelion, 1989), to model earthquake activity. In the field of rock mechanics, AE methods have been implemented to address problems such as rock burst predictions, hydraulic fracturing, mine pillar stress and deformation, rock mass stability, and the velocity of groundwater movement (Glaser and Nelion, 1989).

In India, acoustic emission studies related to deformation processes in brittle rock and failure pre-cursors of rock burst prone rock have been done (Rao, 1992). Central Mining Research Institute, Regional Centre, Nagpur too, has conducted field oriented research studies using AE tool for rock stability assessment. Such studies were successfully completed in Khetri Copper mines in Rajasthan (CMRI, 2002).

Studies related to rock bolt stability evaluation has also been conducted, wherein attempts were made to correlate AE/MS activity with various anchorage-testing parameters (Unal and Hardy, 1982). Laboratory studies of AE prior to uniaxial compressive rock failure reveal significant information about the stress state, and about the stage of rock disintegration (Rudajev et al., 2000). AE tool has also been used for studying rock damage behaviour using rock damage parameter as provided by Seto et al. (1996).

A basic parameter required in rock mechanics design is the state of insitu stress. Conventional measurement of this parameter is normally accomplished using various over-coring, flat-jack and hydro-fracturing techniques. Laboratory investigation reveal that AE generated in a loaded rock gives an idea of the cracking process in it (Li and Norlund, 1993). It has been observed that, when rocks are subjected to cyclic loading and unloading, AE are detected only when the maximum stress is exceeded from the previous loading cycle. Such an AE phenomenon is known as ‘Kaiser Effect’. This effect was first observed in metals by Kaiser (1950). The following paper presents the outcomes of the AE study conducted to determine the insitu stress of rock using AE phenomenon like Kaiser and Felicity effect.

2. TERMINOLOGY

Acoustic emission parameters which were used for the analysis are as mentioned below.

Peak amplitude - This can be related to the intensity of the source in the rock producing an acoustic emission.
Threshold - Amplitude set by the user to filter out unwanted noise.
Ringdown counts - The number of times a signal crosses a preset threshold datum.
Event duration - Time till an event first crosses the preset threshold & the waveform amplitude remaining above the threshold.
Rise time - It measures the time it takes to reach the peak amplitude.
Peak to counts - Counts that attains peak amplitude value.

3. EXPERIMENTAL SET-UP

3.1 Rock Core Samples

Rock cores were obtained from different vertical boreholes from a coal mine and a hydroelectric project. Table 1 details the type of rock, the depth from which the samples are taken along with the dimension of the rock samples to be tested. In this test UTM is used to provide cyclic loading and unloading to the rock samples and at no stage the UCS of the sample is required to be determined. Samples 'G1', 'G2' and 'G3' were prepared from the same core and so are from the same depth. Samples 'J3' and 'J4' are also obtained from the same depth whereas 'J1' and 'J2' are from different depths (Table 1). The rock samples were dried for 4 minutes in a pre-heated oven up to a maximum temperature of 100ºC, without rendering the sample completely dry. This was done to remove the excess moisture, which might have penetrated into the sample during its preparation from rock cores.

Table 1 - Rock sample details

S. No.	Sample No.	Location	Rock Type	Depth, m	Length, mm	Diameter, mm
1.	G1	Ghatghar Hydel Project	Compact Basalt	263	90.94	42.13
2.	G2	--do--	--do--	263	99.41	42.32
3.	G3	--do--	--do--	263	98.85	42.15
4.	J1	Jhanjra, ECL	Medium grained sandstone	88.51	103.94	53.74
5.	J2	--do--	Coarse grained sandstone	85.46	106.76	52.12
6.	J3	--do--	--do--	84.11	104.94	54.50
7.	J4	--do--	--do--	84.11	103.18	54.59

3.2 AE Instrumentation

The acoustic emission (AE) signatures were monitored by using MISTRAS system (Make: Physical Acoustic Corp., UK). The block diagram of AE equipment is shown in Fig.1. The system consisted of basic 2-channels and includes two transducers, two pre-amplifiers & an AEDSP board installed in a personal computer. In the tests conducted only one channel or sensor was used. The general features of the AE instrument and the hardware setup menu are tabulated in Tables 2 and 3 respectively.

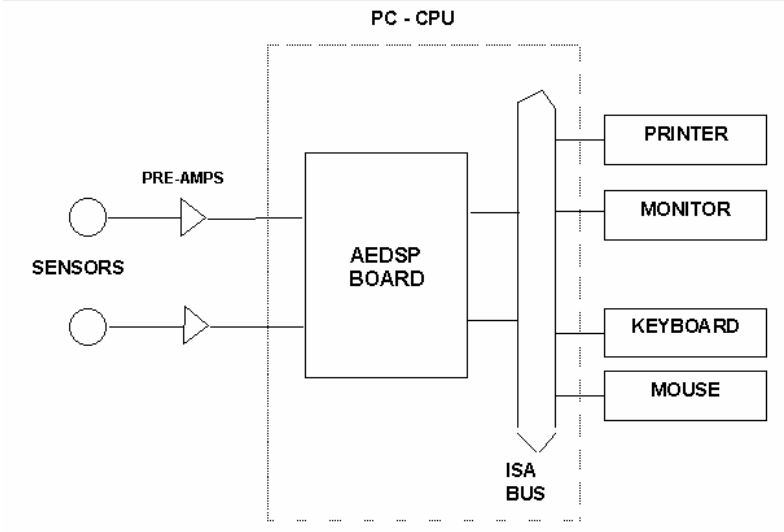

Fig. 1 – Block diagram of AE monitoring system

Table.2 - General features of AE instrument

Features	Number	Specification/Function
Sensors/Transducers	01	Piezoelectric crystal, Resonant Frequency – 60kHz Low Frequency Sensors – 50 to 200 kHz
Pre-amplifiers	01	Gain – 40 dB to 60 dB Bandpass Filter – 10 kHz to 1.2MHz Input – Single or Differential selectable
AEDSP Card/Board	01	Hardware interface. Performs digital signal processing
MISTRAS	01	Software interface for acquiring, storing and analyzing the Acoustic Emissions

Table 3 - Hardware setup menu

Sensor	Preamp (dB)	Threshold (dB)	PDT (μs)	HDT (μs)	HLT (μs)
I	40	30	100	200	1000

One PAC-R6D low frequency transducers was used for AE monitoring. The key element in a resonant transducer was a piezoelectric crystal. The crystal was housed in a suitable enclosure with a wear plate and a connector. The resonant frequency of the sensor used was 60 kHz with a part range. Low frequency sensor (50-200 kHz) was used for the tests. The pre-amplifiers typically provided a gain of 100 (40dB) and included a high-pass or band-pass filter to eliminate the mechanical & acoustical background noise that prevails at low frequencies.

The AE signals from the rocks were converted into electrical signals by the sensors, amplified to usable voltage levels by the pre-amplifiers and measured in the AEDSP-32/16 card, each which contained two full digital waveform & signal processing AE channels. The data from each AEDSP-32/16 card was passed to a host PC, through the PC's ISA bus, where the data was stored, displayed to the operator and analysed.

4. CYCLIC LOADING AND UNLOADING

The experimental setup used for testing of samples is illustrated in Figure 2. Each sample was uniaxially loaded and unloaded till the rock sample failed with AE transducers continuously monitoring the acoustic events throughout all the loading and unloading cycles. Considering the rock type, the loading and unloading cycle rate was decided. In case of Ghatghar samples, the loading cycle rate was 1500 kgs per cycle with 100 kg load being applied every 10 seconds. The unloading cycle rate for the samples was 500 kgs per cycle with 500 kg load being reduced in 10 seconds (Table 4a).

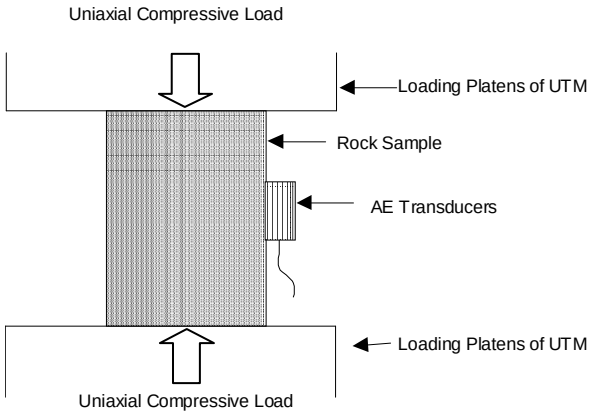

Fig. 2 - Laboratory Set-up for testing of rock samples

Similarly, the loading cycle rate for Jhanjra samples was 600 kgs load per cycle with 100 kg load every 10 seconds and the unloading cycle rate was 200 kgs per cycle with 200 kgs load reduction in 10 seconds (Table 4b).

Table 4a - Loading & unloading cycle rate for Ghatghar Project
(Loading Cycle Rate = 1500 kgs/cycle @ 100 kgs / 10 seconds & Unloading Cycle Rate = 500 kgs/cycle @ 500 kgs / 10 seconds)

Time (sec.)	Cumulative Time (sec.)	Uniaxial Compressive Load (Kg.)	Cumulative Load (Kg.)	Remarks
10	10	100	100	1st Loading Cycle
10	20	100	200	1st Loading Cycle
10	30	100	300	1st Loading Cycle
10	40	100	400	1st Loading Cycle
10	50	100	500	1st Loading Cycle
10	60	100	600	1st Loading Cycle
10	70	100	700	1st Loading Cycle
10	80	100	800	1st Loading Cycle
10	90	100	900	1st Loading Cycle
10	100	100	1000	1st Loading Cycle
10	110	100	1100	1st Loading Cycle
10	120	100	1200	1st Loading Cycle
10	130	100	1300	1st Loading Cycle
10	140	100	1400	1st Loading Cycle
10	150	100	1500	1st Loading Cycle
10	160	(-)500	1000	1st Unloading Cycle
10	170	100	1100	2nd Loading Cycle & so on

Table 4b - Loading & unloading cycle rate for Jhanjra Project
(Loading Cycle Rate = 600 kgs/cycle @ 100 kgs / 10 seconds &. Unloading Cycle Rate = 200 kgs/cycle @ 200 kgs / 10 seconds)

Time (sec)	Cumulative Time (sec)	Uniaxial compressive Load (Kgs)	Cumulative Load (Kgs)	Remarks
10	10	100	100	1st Loading Cycle
10	20	100	200	1st Loading Cycle
10	30	100	300	1st Loading Cycle
10	40	100	400	1st Loading Cycle
10	50	100	500	1st Loading Cycle
10	60	100	600	1st Loading Cycle
10	70	(-) 200	400	1st Unloading Cycle
10	80	100	500	2nd Loading Cycle & so on

When load is constantly applied to a rock sample, after a specific stress level, there is a sharp decrease in AE signals. This indicates that at this point even with increase in load on the sample, the acoustic emissions die down. At this juncture, the sample is unloaded and relieved of any external stress, followed by another loading cycle. The sample will finally fail when its crushing strength is exceeded. Within the samples crushing strength, a number of loading and unloading cycles is monitored. Hence, as is evident from Tables 4a & 4b, the loading and unloading rates differ for both Ghatghar & Jhanjra samples.

5. INSITU STRESS MEASUREMENT

Uniaxial load was applied to the sample with 100 kg load being applied in every 10 seconds. After 150 seconds (end of 1st loading cycle) i.e. at 1500 kg load, the sample was unloaded in the next 10 seconds by 500 kgs. In other words, at 160 seconds the total load on the sample was 1000 kgs. Again the second loading cycle started with 100 kg load increment being applied again at every 10 seconds. Acoustic emissions continuously occurred during the first loading cycle till 150 seconds and 1500 kgs load (Fig. 3).

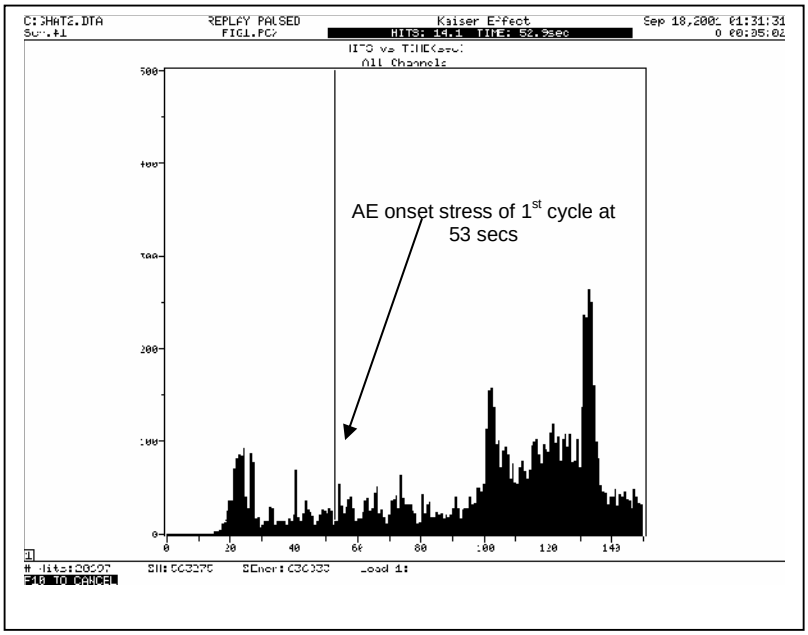

Fig. 3 - First Loading cycle up to 1500 kg load of 'G1' sample

The maximum load on the sample in the first cycle was 1500 kgs. No acoustic emissions were observed in between 150 seconds and 160 seconds (i.e. first unloading cycle), wherein the load was reduced from 1500 kgs to 1000 kgs. In the second loading, starting from 1000 kgs, the load was increased. No acoustic emissions were observed till the load exceeded the maximum load of the first cycle (i.e. 1500 Kgs) corroborating the 'Kaiser Effect'. However, it was observed that at higher stress level, onset of continuous AE did not occur at the maximum load of

previous cycle, but at a load just before the maximum of the previous cycle. This AE phenomenon is known as 'Felicity Effect'.

Felicity Ratio is defined as below

Felicity Ratio = (AE onset stress) / (Maximum stress of previous cycle)

The rock samples were subjected to six loading and unloading cycles (Figs. 4 to 6), and the felicity ratios of last five cycles were determined (Table 5).

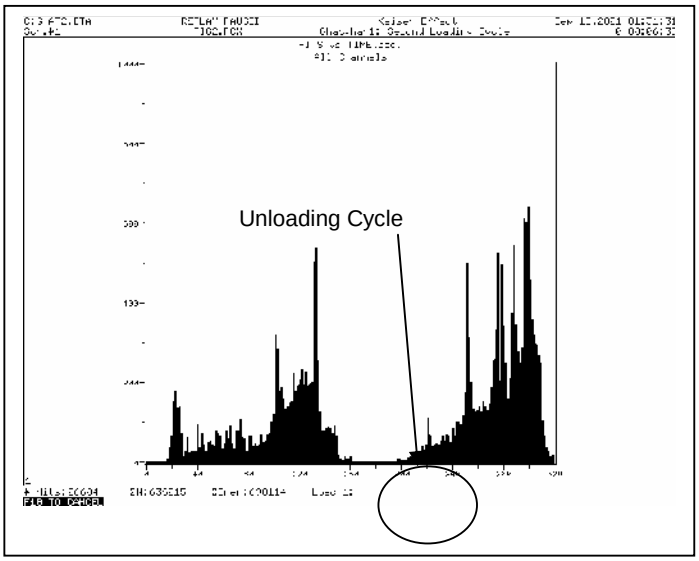

Fig. 4 - Second Loading cycle of 'G1' sample showing emissions when load exceeds previous cycle (Kaiser Effect)

$$\text{Felicity Ratio } (2^{nd} \text{ cycle}) = \frac{\text{AE onset stress of } 2^{nd} \text{ cycle } (= 9.5 \text{ MPa})}{\text{Max. stress of } 1^{st} \text{ cycle } (= 10.55 \text{ MPa})} = 0.90$$

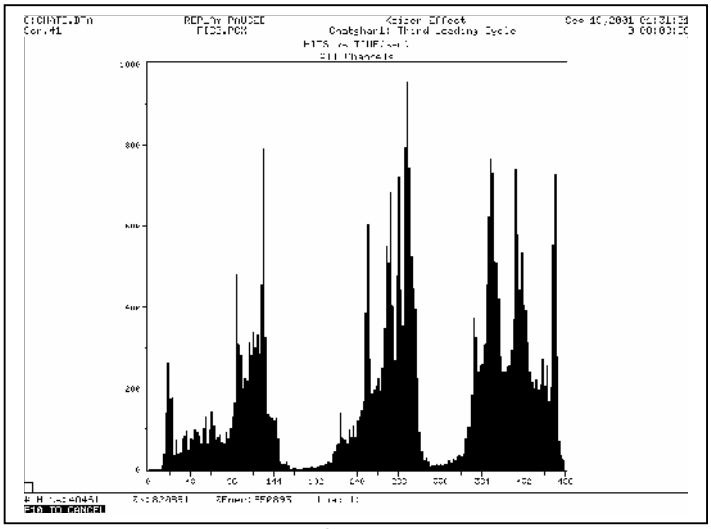

Fig. 5 – Third cyclic loading of 'G1' sample showing Kaiser effect

Table 5 - Felicity Ratio (FR) details of different cycles

Sample No.	2nd Cycle			3rd Cycle			4th Cycle			5th Cycle			6th Cycle			Avg. FR
	AE onset stress (Time, sec)	Max. stress of previous cycle, MPa	FR2	AE onset stress (time, s)	Max. stress of previous cycle, MPa	FR3	AE onset stress (time, s)	Max. stress of previous cycle, MPa	FR_4	AE onset stress (time, s)	Max. stress of previous cycle, MPa	FR_5	AE onset stress (time, s)	Max. stress of previous cycle, MPa	FR_6	
G1	9.5 (195)	10.55	0.9	15.76 (344)	17.59	0.896	21.8 (494)	24.63	0.885	28.71 (648)	31.67	0.906	37.16 (828)	38.7	0.96	0.9094
G2	10.04 (204)	10.46	0.96	16.04 (350)	17.43	0.92	22.73 (506)	24.41	0.931	30.55 (678)	31.38	0.97	37.73 (841)	38.36	0.98	0.9522
G3	9.63 (197)	10.54	0.91	16.59 (356)	17.57	0.944	23.9 (520)	24.6	0.971	29.53 (660)	31.64	0.93	36.14 (814)	38.67	0.934	0.9378
J1	2.33 (84)	2.59	0.9	4.06 (154)	4.32	0.94	5.32 (213)	6.05	0.878	7.22 (287)	7.78	0.927	8.78 (353)	9.516	0.922	0.9134
J2	2.34 (89)	2.76	0.85	4.09 (149)	4.59	0.89	6.11 (223)	6.43	0.95	7.58 (285)	8.27	0.916	9.7 (361)	10.11	0.959	0.913
J3	2.18 (82)	2.52	0.866	3.82 (151)	4.2	0.91	5.46 (220)	5.88	0.928	7.15 (290)	7.57	0.944	8.53 (353)	9.25	0.922	0.914
J4	2.30 (85)	2.51	0.916	3.94 (154)	4.19	0.94	5.07 (211)	5.86	0.864	6.87 (284)	7.54	0.911	8.55 (354)	9.22	0.927	0.9116

$$\text{Felicity Ratio } (3^{rd} \text{ cycle}) = \frac{\text{AE onset stress of } 3^{rd} \text{ cycle } (=15.76 \text{ MPa})}{\text{Max. stress of } 2^{nd} \text{ cycle } (=17.59 \text{ MPa})} = 0.896$$

Figure 6 illustrates six loading and unloading cycles of the samples, based on which the Felicity ratios were determined.

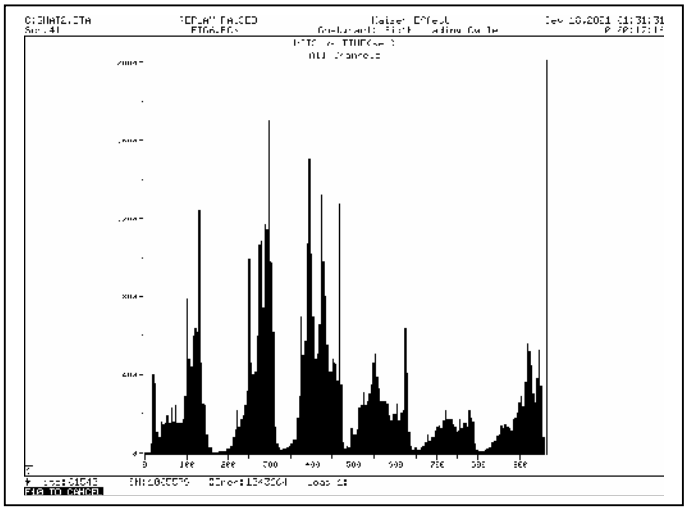

Fig. 6 - Acoustic signatures of six loading & unloading cycles of 'G1' sample

Thus, the felicity ratio for a particular rock at a given depth was known by averaging the felicity ratios of all five cycles. From Fig. 3, the acoustic emission onset stress of 1^{st} cycle was determined. Acoustic emissions are observed (Fig. 3) as soon as the sample is subjected to compression loading. Many acoustic emissions observed may be due to collapsing of pore spaces and material adjustment of grains in the sample. In the first cycle, the AE onset stress has to be determined correctly after filtering out the unwanted noise. The proper detection of AE onset stress depends, to a large extent, on the experience of the user. In the first loading cycle the maximum stress of the previous cycle or in other words, the existing insitu stress was determined by

$$\text{Felicity Ratio } (1^{st} \text{ cycle}) = \frac{\text{AE onset stress of } 1^{st} \text{ cycle (known)}}{\text{Max. stress prior to } 1^{st} \text{ cycle (to be determined)}}$$

or insitu stress

Similarly, the Felicity ratio of Jhanjra samples was determined. Figure 7 shows six cyclic loading pattern and the acoustic emission signatures. Figure 8 shows the expanded view of first loading cycle, which indicates the insitu stress condition prior to loading.

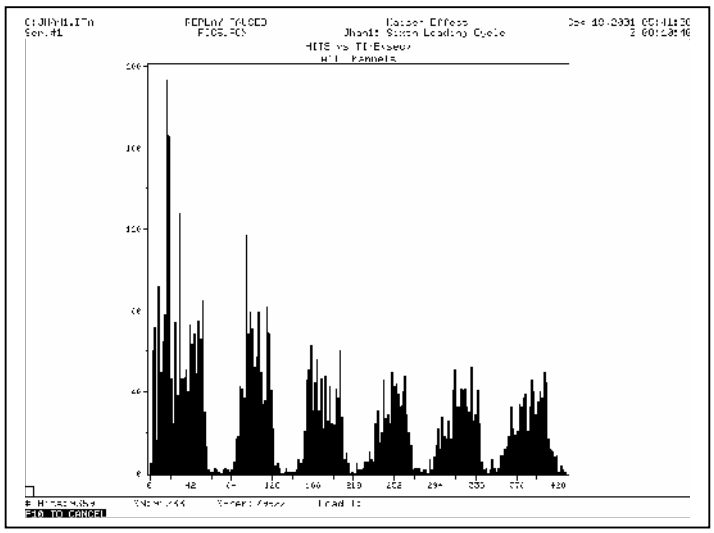

Fig. 7 - Acoustic signatures of cyclic loading and unloading of 'J1' sandstone samples

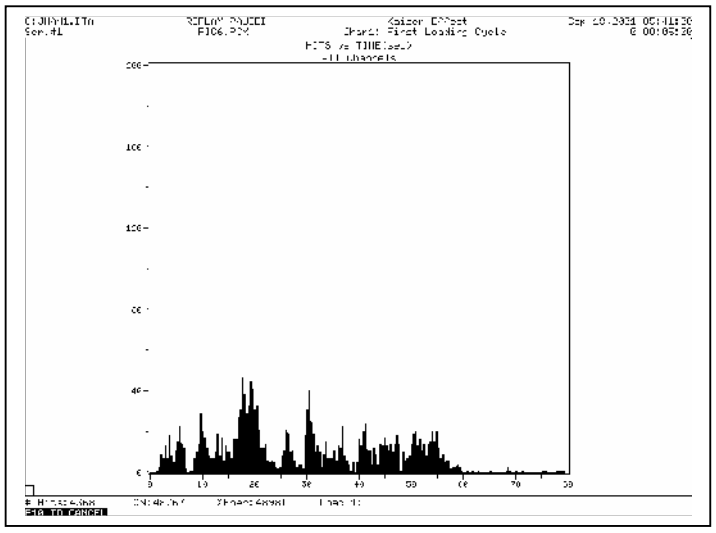

Fig. 8 - First cycle acoustic signatures of 'J1' sandstone sample

Table 5 tabulates the details of cyclic loading of all the samples, which led to the determination of the average felicity ratio of each sample. The insitu stress determined after due analysis of the first cycle are detailed in Table 6.

6. ANALYSIS & DISCUSSIONS

Insitu stress determined in all the samples mentioned in Table 6 were from vertically drilled borehole core specimens. Samples were prepared from these cores and loaded in an axial direction. The stress determined in all the cases was the vertical stress at different depths. Felicity ratio as indicated from AE signals

depends to a large extent on the maximum stress in rock mass during the previous cycle. In the first cycle, felicity ratio was used to determine the maximum insitu vertical stress, which might be present in the sample. Rocks have a property of retaining the acoustic signatures of the maximum stress state which it has undergone in its whole history and it is only when the stress exceeds the maximum stress, acoustic signals are again emitted. Thus, the stress determined with the help of AE tool in laboratory gives the value of the maximum vertical insitu stress of the rock mass and may not necessarily point to the current or existing insitu stress state.

Table 6 - Indirect determination of insitu stress from 1st Cycle

Sample No.	Felicity ratio	Onset stress of 1st cycle, MPa (time, secs)	Calculated maximum stress of previous cycle (Insitu stress), MPa	Average insitu stress by AE technique, MPa
G1	0.9094	3.73 (at 53 secs)	4.101	4.054 (Avg. of G1, G2 & G3)
G2	0.9522	3.90 (at 56 secs)	4.095	
G3	0.9378	3.72 (at 53 secs)	3.966	
J1	0.9134	1.557 (at 36 secs)	1.704	1.588 (Avg. of J1, J2, J3 & J4)
J2	0.913	1.517 (at 33 secs)	1.66	
J3	0.914	1.261 (at 30 secs)	1.38	
J4	0.9116	1.467 (at 35 secs)	1.609	

Comparisons of the insitu vertical stress results as obtained using AE tool and theoretical calculation are given in Table 7.

Table 7 – Vertical insitu stress from acoustic emission (AE) technique and conventional theoretical method

	Vertical Insitu Stress, MPa				
	Ghatghar Sample	Jhanjra Sample 1	Jhanjra Sample 2	Jhanjra Sample 3	Jhanjra Sample 4
Depth, m	263	88.51	85.46	84.11	84.11
A E Tool	4.054	1.704	1.66	1.38	1.609
Other methods	6.5 (theoretical)	1.91 (theoretical)	1.84 (theoretical)	1.81 (theoretical)	1.81 (theoretical)

The insitu stress values obtained by hydro-fracturing method for Ghatghar sample was found out to be 4.6 MPa , which is close to insitu stress obtained from AE technique (Table 7). This is not matching with the theoretical value of 6.5MPa. Insitu stress values using hydro-fracturing techniques or any other conventional field methods were not available for Jhanjra samples, at the depth from where samples were tested using acoustic emission tool. Hence, theoretical values ($\sigma_v=\rho gh$) were considered for comparison (Table 7). For rocks of coal bearing formations, as in case of Jhanjra samples, it was found that the maximum vertical insitu stress estimated by the theoretical formula for coal bearing rocks is close to the values obtained by acoustic emission technique.

Thus, Table 7 shows a variation in comparison of vertical insitu stress values obtained from AE technique and theoretical method in case of the samples of two projects. This may be because the samples of the two projects are from different geological environment and depths.

It has been found from the literatures that the insitu stress value obtained from theoretical method may not hold good in many conditions owing to the effects of geological structures. The vertical stress might vary along a horizontal plane cutting through a succession of rigid and compliant beds folded into synclines and anticlines (Goodman, 1980). The study presented here supports the findings of Goodman, (1980).

7. CONCLUSIONS

Acoustic emission technique has been found a suitable alternative tool to obtain the maximum vertical insitu stress. Results indicate that vertical stress at the same depth with acoustic emission method is near to the insitu stress values as determined by other conventional methods. Moreover, the results also indicate that the applicability of theoretical formulae does not hold good for rock samples having geological heterogeneity, as is found in Ghatghar samples (Table 7). The maximum vertical insitu stress values with acoustic emission technique for such geologically heterogencous rocks were found to be in line with the results obtained by hydro-fracturing technique. Researchers in the past have compared insitu stresses obtained by acoustic emission technique with overcoring methods. They too have found that the two techniques appear to provide results, which are in reasonable agreement, with acoustic emission technique giving somewhat higher value (Hardy, 1981). The present study thus provided an indirect evaluation of insitu stresses, thereby indicating potential applicability of acoustic emission technique.

Acknowledgements

The authors are thankful to Dr. P. R. Sheorey, Former Dy. Director, CMRI and Mr. A K Ghosh, Scientist ‘F’, CMRI for rendering their views and help in the above study. Thanks are also due Mr. V. S. Jaipal, Scientist ‘B’, CMRI, for his immense help during the study.

References

CMRI Internal Report (2002), Acoustic studies to investigate into the crown pillar stability at 300m level of Khetri mine, Hindustan Copper Limited, No.GC/MT/60/2000-2001, pp.1-21.

Glaser, S. D. and Nelion, P. P. (1989), Analysis of acoustic emission waveforms produced by rock during controlled fracture propagation, Fracture of concrete & rock - Recent development, Elsevier Applied Sciences, pp.111-120

Goodman, R. E. (1980), “Introduction to rock mechanics”, Publ. John Wiley & Sons, pp. 99-101

Hardy, H. R., Jr. (1981), “Application of acoustic emission technique to rock and rock structures: A state-of-the-art review”, Symposium on acoustic emission in

Geotechnical Engineering Practice, ASTM, Philadelphia, Pennsylvania, USA, pp.4-92.

Kaiser, E. J. (1950), A study of acoustic phenomena in tensile test, Doctoral thesis, Technische Hochshile Munchen, Germany, pp. 1-30.

Li, C. and Norlund, E. (1993), Assessment of damage in rock using the Kaiser effect of acoustic emission, Intl. Journal of Rock Mechanics & Mining Sciences, Vol. 30, No. 7, pp. 943-946.

Rao, M. V. M. S. (1992), Acoustic emission activity & failure precursors in some of the rocks of Kolar gold mines, Proc. 6th Natl. Symposium on Rock Mechanics, Bangalore, pp. 1-10

Rudajev, V., Vilhelm, J. and Lokajicek, T. (2000), Laboratory studies of acoustic emission prior to uniaxial compressive rock failure, Intl. Journal of Rock Mechanics & Mining Sciences, Vol. 37, pp. 699-704.

Seto, M., Nag D. K. and Vutukuri V. S. (1996), Application of acoustic emission technique to evaluate rock mass damage, Trends in NDE Science & Technology, Proc. of 14th world conference on NDT, New Delhi, Vol. 4, pp. 2451-2454.

Unal, E. and Hardy, H. R. (1982), Application of acoustic emission technique in the evaluation of rock bolt stability, Proc. 3rd Conference on acoustic emission / microseismic activity in geologic structures & materials, Trans Tech Publication, Claisthal, Germany, pp 814.